Hindawi Publishing Corporation
Advances in High Energy Physics
Volume 2015, Article ID 726393, 7 pages
http://dx.doi.org/10.1155/2015/726393

Research Article

Next-to-Leading Order Differential Cross Sections for J/ψ, $\psi(2S)$, and Υ Production in Proton-Proton Collisions at a Fixed-Target Experiment Using the LHC Beams

Yu Feng and Jian-Xiong Wang

Institute of High Energy Physics, Chinese Academy of Sciences, P.O. Box 918(4), Beijing 100049, China

Correspondence should be addressed to Yu Feng; yfeng@ihep.ac.cn

Received 17 April 2015; Accepted 4 June 2015

Academic Editor: Cynthia Hadjidakis

Using nonrelativistic QCD (NRQCD) factorization, we calculate the yields for J/ψ, $\psi(2S)$, and $\Upsilon(1S)$ hadroproduction at $\sqrt{s}$ = 72 GeV and 115 GeV including the next-to-leading order QCD corrections. Both these center-of-mass energies correspond to those obtained with 7 TeV and 2.76 TeV nucleon beam impinging a fixed target. We study the cross section integrated in p_t as a function of the (center-of-mass) rapidity as well as the p_t differential cross section in the central rapidity region. Using different NLO fit results of the NRQCD long-distance matrix elements, we evaluate a theoretical uncertainty which is certainly much larger than the projected experimental uncertainties with the expected 20 fb^{-1} to be collected per year with AFTER@LHC for pp collision at the center of mass energy $\sqrt{s} \simeq 115$ GeV.

1. Introduction

Nonrelativistic quantum chromodynamics (NRQCD) [1] is the most systematic factorization scheme to describe the decay and production of heavy quarkonia. It allows one to organize the theoretical calculations as double expansions in both the coupling constant α_s and the heavy-quark relative velocity v. In the past few years, significant progress has been made in next-to-leading order (NLO) QCD calculations based on NRQCD. Calculations and fits of NRQCD long-distance matrix elements (LDMEs) for both the J/ψ yield and polarization in hadroproduction have been carried out [2–6] as well as for Υ hadroproduction [7, 8]. Using these LMDEs, one can in principle predict the transverse momentum p_t differential cross section at any energies. In addition, in a recent study [9], we have discussed the implication of these fits on the energy dependence of the cross sections integrated in p_t.

In this paper, we predict these differential cross sections for the kinematics of a fixed-target experiment using the LHC beams (AFTER@LHC) [10]. In practice, 7 TeV protons on targets yield to a c.m.s energy close to 115 GeV and 72 GeV for 2.76 TeV nucleons (as in the case of a Pb beam). This corresponds to a range very seldom explored so far, significantly higher than that at CERN-SPS and not far from BNL-RHIC. With the typical luminosity of the fixed-target mode, which allows for yearly luminosities as large as 20 fb^{-1} in pp collision at $\sqrt{s} \simeq 115$ GeV, AFTER@LHC is expected to be a quarkonium and heavy-flavor observatory [10, 11]. In general, the opportunities of a fixed-target experiment using the LHC beam for spin and heavy-ion physics are discussed in [10, 12–14]. With the calculation at $\sqrt{s} = 72$ GeV, which is supposed to be a baseline rate where nuclear effects would be added, we confirm that charmonium yields can easily reach 10^9 per year and 10^6 for bottomonium at $\sqrt{s} \simeq 115$ GeV.

2. Next-to-Leading Order Calculation

Following the NRQCD factorization formalism [1], the cross section for quarkonium hadroproduction H can be expressed as

$$d\sigma\left[pp \longrightarrow H + X\right] = \sum_{i,j,n} \int dx_1 dx_2 G_p^i G_p^j d\hat{\sigma}\left[ij \longrightarrow \left(Q\overline{Q}\right)_n X\right] \left\langle \mathcal{O}_n^H \right\rangle, \quad (1)$$

where p is either a proton or an antiproton, $G_p^{i(j)}$ is the parton distribution function (PDF) of p, the indices i, j run over all possible partonic species, and n denotes the color, spin, and angular momentum states of the intermediate $Q\overline{Q}$ pair. For ψ and Υ, namely, the ${}^3S_1$ quarkonium sates, their leading CO states of relative order $\mathcal{O}(v^4)$ are ${}^1S_0^{[8]}$, ${}^3S_1^{[8]}$, and ${}^3P_J^{[8]}$. Along with the CS transition ${}^3S_1^{[1]}$, we call the total CS + CO contributions as direct production. The short-distance coefficient (SDC) $d\hat{\sigma}$ will be calculated perturbatively, while the long-distance matrix elements (LDMEs) $\langle \mathcal{O}_n^H \rangle$ are governed by nonperturbative QCD effects.

Now let us take a look at the parton level processes relevant to this work. As it is well known, the CO contributions to hadroproduction appear at α_s^2 [15] and their Born contributions are

$$\begin{aligned} q + \overline{q} &\longrightarrow Q\overline{Q}\left[{}^3S_1^{[8]}\right], \\ g + g &\longrightarrow Q\overline{Q}\left[{}^1S_0^{[8]}, {}^3P_{J=0,2}^{[8]}\right], \end{aligned} \tag{2}$$

where $q(\overline{q})$ denotes the light quarks (antiquarks).

Up to α_s^3, QCD corrections include real and virtual corrections. One inevitably encounters ultra-violet (UV), infrared (IR), and Coulomb divergences when dealing with the virtual corrections. UV divergences from self-energy and triangle diagrams are canceled upon the renormalization procedure. For the real emission corrections, three kinds of processes should be considered:

$$\begin{aligned} g + g &\longrightarrow Q\overline{Q}\left[{}^3S_1^{[1]}, {}^1S_0^{[8]}, {}^3S_1^{[8]}, {}^3P_{J=0,2}^{[8]}\right] + g, \\ g + q\,(\overline{q}) &\longrightarrow Q\overline{Q}\left[{}^1S_0^{[8]}, {}^3S_1^{[8]}, {}^3P_{J=0,2}^{[8]}\right] + q\,(\overline{q}), \\ q + \overline{q} &\longrightarrow Q\overline{Q}\left[{}^1S_0^{[8]}, {}^3S_1^{[8]}, {}^3P_{J=0,1,2}^{[8]}\right] + g, \end{aligned} \tag{3}$$

some of which involve IR singularities in phase space integration and we adopt the two-cutoff phase space slicing method [16] to isolate these singularities by introducing two small cutoffs, δ_s and δ_c. For technical details, we refer readers to [17, 18].

One has to note that in (3), the ${}^3S_1^{[1]}$ production in gg fusion is not really correction. Strictly speaking, it is only the Born-order contribution for hadroproduction with a jet. In fact, all the real emission processes in (3) will be taken as Born-order contributions of quarkonium-jet production.

As regards to the p_t dependent differential cross section, and the QCD NLO corrections in this case are up to α_s^4, which involves the real emission processes

$$\begin{aligned} g + g &\longrightarrow \left(Q\overline{Q}\right)_n + g + g, \\ g + g &\longrightarrow \left(Q\overline{Q}\right)_n + q + \overline{q}, \\ g + q\,(\overline{q}) &\longrightarrow \left(Q\overline{Q}\right)_n + g + q\,(\overline{q}), \\ q + \overline{q} &\longrightarrow \left(Q\overline{Q}\right)_n + g + g, \\ q + \overline{q} &\longrightarrow \left(Q\overline{Q}\right)_n + q + \overline{q}, \\ q + \overline{q} &\longrightarrow \left(Q\overline{Q}\right)_n + q' + \overline{q}', \\ q + q &\longrightarrow \left(Q\overline{Q}\right)_n + q + q, \\ q + q' &\longrightarrow \left(Q\overline{Q}\right)_n + q + q', \end{aligned} \tag{4}$$

where q, q' denote light quarks with different flavors and $(Q\overline{Q})_n$ can be either ${}^3S_1^{[1]}$, ${}^1S_0^{[8]}$, ${}^3S_1^{[8]}$, or ${}^3P_J^{[8]}$. One can find the details of such computations at this order in [18, 19] and some examples in [2, 3, 6–8].

All of these calculations are made with the newly updated Feynman Diagram Calculation package [20].

3. Constrains on the LDMEs

The color-singlet (CS) LDMEs are estimated from the wave functions at the origin by $\langle \mathcal{O}^H({}^3S_1^{[1]}) \rangle = (3N_c/2\pi)|R_H(0)|^2$, where the wave functions are obtained via potential model calculation [21]. This gives $|R_{J/\psi}(0)|^2 = 0.81\,\mathrm{GeV}^3$, $|R_{\psi(2S)}(0)|^2 = 0.53\,\mathrm{GeV}^3$, and $|R_{\Upsilon(1S)}(0)|^2 = 6.5\,\mathrm{GeV}^3$. In the following, we will refer to this contribution as the CSM results when performed separately.

The color-octet (CO) LDMEs can only be extracted from data. As for now, SDC are known up to NLO accuracy and the fits of LDMEs can be thus performed at NLO. However, different results are obtained when different dataset is used. We made a selection of these fits in order to assess the theoretical uncertainty induced by the LDMEs. We briefly discuss below these different fit results.

In the J/ψ case, seven groups of LDMEs [2, 5, 6, 22–25] are collected in Table 1. They are extracted by fitting the data of hadroproduction yield [2] or combined with polarization [5, 6] on pp collisions. The first one [22] was based on a wider set of data including ep and $\gamma\gamma$ system with $p_t > 1\,\mathrm{GeV}$. In [5, 6], the data with $p_t < 7\,\mathrm{GeV}$ are excluded in their fit. The fit in [23, 24] took the η_c measurement ($p_t \geq 6\,\mathrm{GeV}$) into consideration. Only one of them is used [24] since their results are almost the same. The last one incorporates the leading-power fragmentation corrections together with the QCD NLO corrections, which results in a different SDC and may result in different LDMEs. In [2], Ma et al. fit the data with $p_t > 7\,\mathrm{GeV}$ by two linear combinations of LDMEs:

$$\begin{aligned} M_{0,r_0}^{J/\psi} &= \left\langle \mathcal{O}^{J/\psi}\left({}^1S_0^{[8]}\right)\right\rangle + \frac{r_0}{m_c^2}\left\langle \mathcal{O}^{J/\psi}\left({}^3P_0^{[8]}\right)\right\rangle, \\ M_{1,r_1}^{J/\psi} &= \left\langle \mathcal{O}^{J/\psi}\left({}^3S_1^{[8]}\right)\right\rangle + \frac{r_1}{m_c^2}\left\langle \mathcal{O}^{J/\psi}\left({}^3P_0^{[8]}\right)\right\rangle, \end{aligned} \tag{5}$$

from which we extract the value of LDMEs by restricting $\langle \mathcal{O}^{J/\psi}({}^1S_0^{[8]}) \rangle$ and $\langle \mathcal{O}^{J/\psi}({}^3S_1^{[8]}) \rangle$ to be positive to get a loose constraint on the $\langle \mathcal{O}^{J/\psi}({}^3P_0^{[8]}) \rangle$ range, from which we choose

Table 1: The values of LDMEs for J/ψ hadroproduction (in units of GeV^3).

References	$\langle \mathcal{O}^{J/\psi}(^3S_1^{[1]})\rangle$	$\langle \mathcal{O}^{J/\psi}(^1S_0^{[8]})\rangle$	$\langle \mathcal{O}^{J/\psi}(^3S_1^{[8]})\rangle$	$\langle \mathcal{O}^{J/\psi}(^3P_0^{[8]})\rangle/m_Q^2$
Butenschoen and Kniehl (2011) [22]	1.32	3.0×10^{-2}	1.7×10^{-3}	-4.0×10^{-3}
Chao et al. (2012) [5]	1.16	8.9×10^{-2}	3.0×10^{-3}	5.6×10^{-3}
Ma et al. (2011) [2]	1.16	3.9×10^{-2}	5.6×10^{-3}	8.9×10^{-3}
Gong et al. (2013) [6]	1.16	9.7×10^{-2}	-4.6×10^{-3}	-9.5×10^{-3}
Zhang et al. (2014) [23]	0.24~0.90	$(0.4\sim1.1) \times 10^{-2}$	1.0×10^{-2}	1.7×10^{-2}
Han et al. (2015) [24]	1.16	0.7×10^{-2}	1.0×10^{-2}	1.7×10^{-2}
Bodwin et al. (2014) [25]	0	9.9×10^{-2}	1.1×10^{-2}	4.9×10^{-3}

Table 2: The values of LDMEs for $\psi(2S)$ and $\Upsilon(1S)$ hadroproduction (in units of GeV^3).

H	References	$\langle \mathcal{O}^H(^3S_1^{[1]})\rangle$	$\langle \mathcal{O}^H(^1S_0^{[8]})\rangle$	$\langle \mathcal{O}^H(^3S_1^{[8]})\rangle$	$\langle \mathcal{O}^H(^3P_0^{[8]})\rangle/m_Q^2$
$\psi(2S)$	Gong et al. (2013) [6]	0.76	-1.2×10^{-4}	3.4×10^{-3}	4.2×10^{-3}
	Ma et al. (2011) [2]	0.76	1.4×10^{-2}	2.0×10^{-3}	1.6×10^{-3}
$\Upsilon(1S)$	Gong et al. (2014) [8]	9.28	11.2×10^{-2}	-4.1×10^{-3}	-6.7×10^{-3}
	Han et al. (2014) [26]	9.28	3.5×10^{-3}	5.8×10^{-2}	3.6×10^{-2}
	Feng et al. (2015) [27]	9.28	13.6×10^{-2}	6.1×10^{-3}	-9.3×10^{-3}

the center value in order to obtain the three LDMEs (Ma et al. (2011) in Table 1).

As regards the $\psi(2S)$, only two NLO analyses have been done (see [2, 6]), both of which excluded the data with $p_t < 7$ GeV in their fit. To extract the LDME values from the fit results of Ma et al., the same method is used as for the J/ψ. For $\Upsilon(1S)$, we use three groups of LDMEs [8, 26, 27]. Both of them have exactly accounted for the direct production and the feed-down contributions. In the fit of [26], only the data in $p_t > 15$ GeV region are used, while in [8, 27] the region is $p_t > 8$ GeV. They all describe the high p_t yield data at Tevatron and LHC very well. We gather the LDMEs of $\psi(2S)$ and $\Upsilon(1S)$ in Table 2.

4. Numerical Results

The differential cross sections as a function of (center-of-mass) rapidity and transverse momentum are considered in this section. In both cases, the CTEQ6M parton distribution functions [28] and the corresponding two-loop QCD coupling constants α_s are used. The charm quark mass is set to be $m_c = 1.5$ GeV, while the bottom quark mass is taken to be $m_b = 4.75$ GeV. The renormalization and factorization scales are chosen as $\mu_r = \mu_f = 2m_Q$ for rapidity distribution plots, while for the plots of transverse momentum distribution they are $\mu_r = \mu_f = \mu_T$, with $\mu_T = \sqrt{(2m_Q)^2 + p_t^2}$. The NRQCD scale is chosen as $\mu_\Lambda = m_Q$. It is important to note that different choices of these scales may be adopted which can bring some additional uncertainties in our predictions. We show these uncertainties from the scales combined to those from the quark masses for the plot of the rapidity distribution of the yield (and only for the CO contributions). The scale dependence is estimated by varying μ_r, μ_f, by a factor of 1/2 and 2 with respect to their central values and quark masses varying 0.1 GeV up and down for J/ψ, as well as 0.25 GeV for Υ. Branching ratios are taken from PDG [29], which give $\mathcal{B}[J/\psi \to \mu\mu] = 0.0596$, $\mathcal{B}[\psi(2S) \to \mu\mu] = 0.0079$, and $\mathcal{B}[\Upsilon(1S) \to \mu\mu] = 0.0248$, respectively. The two phase space cutoffs $\delta_s = 10^3$ and $\delta_c = \delta_s/50$ are chosen and the insensitivity of the results on different choices for these cutoffs has been checked.

4.1. $d\sigma/dy$ up to α_s^3. First, we study the p_t-integrated cross section (where the whole p_t region is integrated) as a function of rapidity. The QCD NLO corrections are up to α_s^3 in this case. In Figures 1 and 2, we show the rapidity distribution of direct J/ψ, $\psi(2S)$, and $\Upsilon(1S)$ production cross section at center of mass energy $\sqrt{s} = 72$ GeV and 115 GeV, respectively. We first discuss the "unnormalized" CO channel contributions shown in Figure 1, where the CO LDMEs are set to unity for all three production channels. For $\psi(2S)$, the CSM is different from J/ψ only by a factor, we therefore do not perform it separately. Obviously, the CSM results (red lines) for both J/ψ and $\Upsilon(1S)$ are small compared with the CO channels. The dominant CO channel for J/ψ is $^3P_J^{[8]}$ transition, while for $\Upsilon(1S)$ it is $^1S_0^{[8]}$. Besides, these "unnormalized" contributions for J/ψ display a clear hierarchy, but for $\Upsilon(1S)$, little difference between $^3S_1^{[8]}$ and $^3P_J^{[8]}$ contributions shows up.

Adopting the LDMEs in Tables 1 and 2, we present the rapidity distribution of cross section for various cases in Figure 2. The lines are the central values with different groups of LDMEs, while the colored areas are the uncertainties from scales and quark masses. Only the boundary lines are shown with scales and mass uncertainties. For the J/ψ, six groups of NRQCD results are shown as a band, the boundaries of which has a distance within factor 10. The values of the cross sections are roughly in the region of $10^4 \sim 10^5$ pb. The CSM results are systematically below the full NRQCD band, again by a factor 10. Without a surprise, the CSM seems to be negligible for total NRQCD results. However, some words of cautious are in order here. In fact, as we have

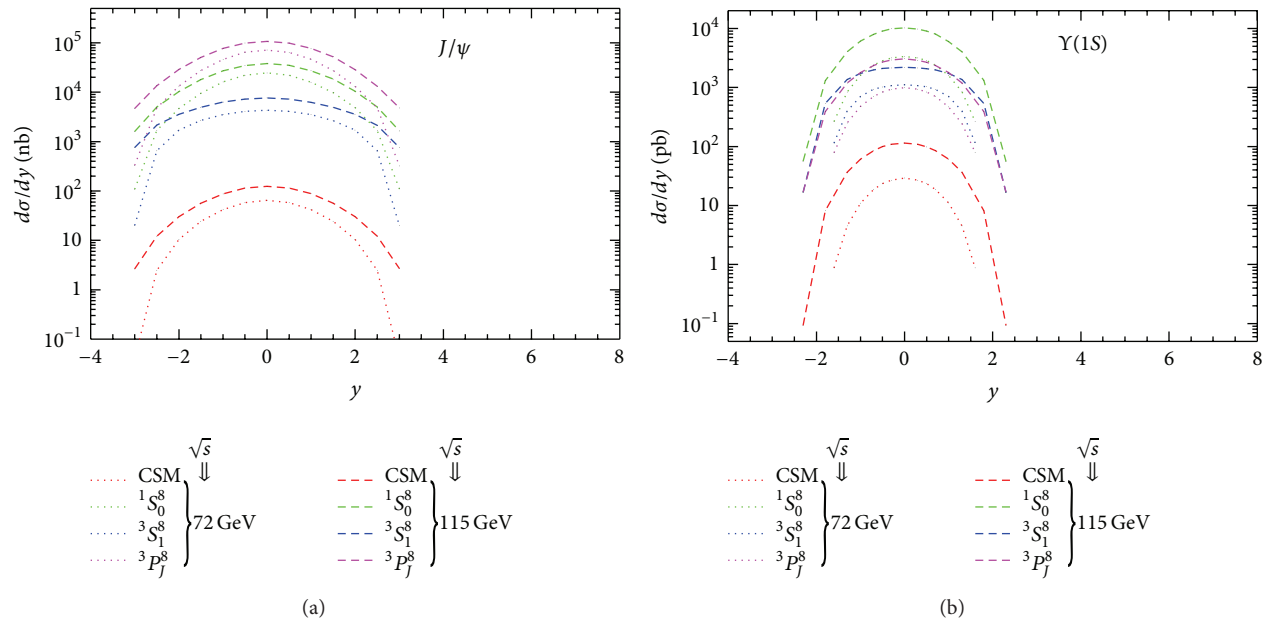

FIGURE 1: The "unnormalized" CO channel contributions for direct J/ψ (a) and $\Upsilon(1S)$ (b) hadroproduction at the c.m.s energy 72 GeV (dot lines) and 115 GeV (dashed lines), respectively. The CO LDMEs for all the channels are set to unity.

discussed in [9], the LO CSM contribution explains the data very well from the RHIC to LHC energies, while the CO LDMEs extracted from p_t-differential NLO correction would lead to p_t-integrated cross sections overshooting the data. Only the fit from Butenschoen and Kniehl [22], including rather low p_t data, provides an acceptable description of the pt-integrated cross section. In other words, most of the predictions in Figure 2 may overshoot the data. One should indeed stress that most of the fits which we used are based on large p_t data, while this rapidity distribution bears on the whole p_t region. We suppose the band from the LDMEs of Butenschoen and Kniehl [22]; namely, the lowest band (red dashed line) would probably give the best prediction of the J/ψ yields, although their LDMEs clearly face difficulty to describe the polarization data. To be complete, let us mention that, following an observations also done in [9], the CSM yield may underestimate the measurements below RHIC energy.

As regards the $\psi(2S)$, two groups of LDMEs lead to a consistent predictions which give a cross section around 10^3 pb at both $\sqrt{s} = 72$ GeV and 115 GeV. Accounting for the uncertainties of the scales and quark masses, the cross sections reach 10^4 pb in the central rapidity region. Nevertheless, these results overestimated the data as discussed in [9].

In the $\Upsilon(1S)$ case, two curves are close and a third one is slightly different. Yet, their difference is only in pb units. At RHIC energies and below [9], this reproduces quite well the $\Upsilon(1S)$ data. This should thus also be the case at the energies considered here.

4.2. $d\sigma/dp_t$ up to α_s^4. Now let us discuss the differential cross sections in the transverse momentum p_t. In Figure 3, the p_t distributions of direct J/ψ, $\psi(2S)$, and $\Upsilon(1S)$ hadroproduction are presented. For J/ψ and $\psi(2S)$, the yields are dominated by the CO contributions, which is larger than that of the CSM at NLO by at least one order of magnitude. The various groups of LDMEs predict J/ψ and $\psi(2S)$ differential yields which are much less spread than for the p_t integrated yields; this is expected since the fits are based on a similar distribution but at different energies. Only the one from [25] (the light blue dot-dashed line) seems to depart from the other ones, being from 2 to 10 times larger in J/ψ case. This may be understood by the fact that the fits in [25] have a different SDC compared with others, which would be the source of the difference.

For $\Upsilon(1S)$, the red dashed and blue dot-dashed lines are almost parallel with a tiny difference, while the green dot line is obviously lower at low p_t region and crosses the other ones as p_t increases. This explains the behavior of $d\sigma/dy$ in Figure 2 with a visible difference between the green curve and the other two.

5. Summary

We evaluated the NLO QCD corrections for the direct J/ψ, $\psi(2S)$, and $\Upsilon(1S)$ production at fixed-target LHC energies. We studied the cross section integrated in p_t as a function of the rapidity as well as the p_t differential cross section in the central rapidity region, including QCD corrections up to α_s^3 and α_s^4 contributions, respectively. To perform a reliable prediction, various sets of NRQCD long-distance matrix elements obtained from different fitting methods are considered as well as the uncertainties from the scales and quark masses. With the typical luminosity of the fixed-target mode, which allows for yearly luminosities as large as 20 fb^{-1} with 7 TeV proton beams, our predictions confirm

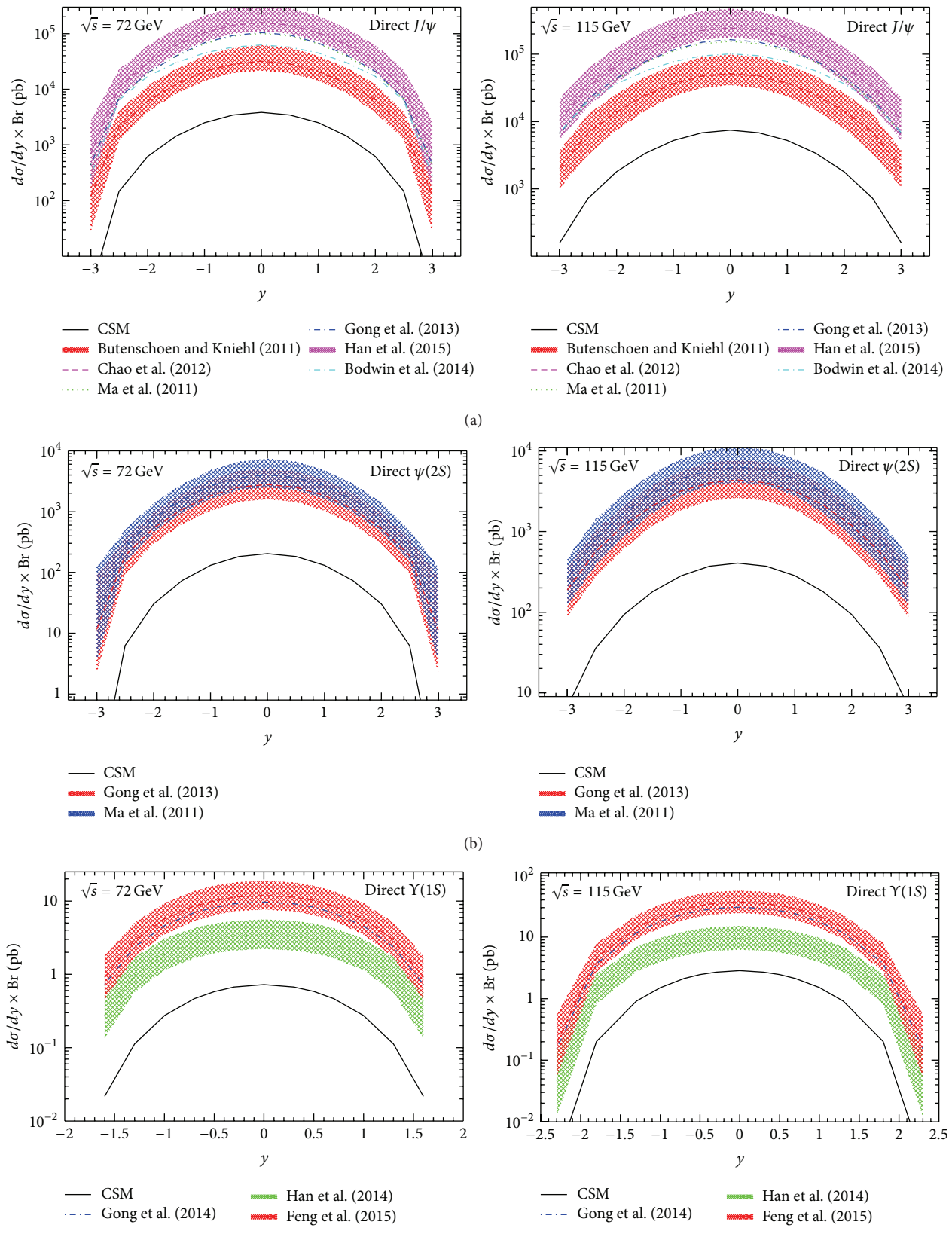

FIGURE 2: Rapidity distribution of differential cross section for direct J/ψ (a), $\psi(2S)$ (b), and $\Upsilon(1S)$ (c) hadroproduction at the center of mass energy $\sqrt{s} = 72$ GeV and $\sqrt{s} = 115$ GeV, respectively. The lines are the uncertainty from LDMEs values while the color areas are scales and masses uncertainties.

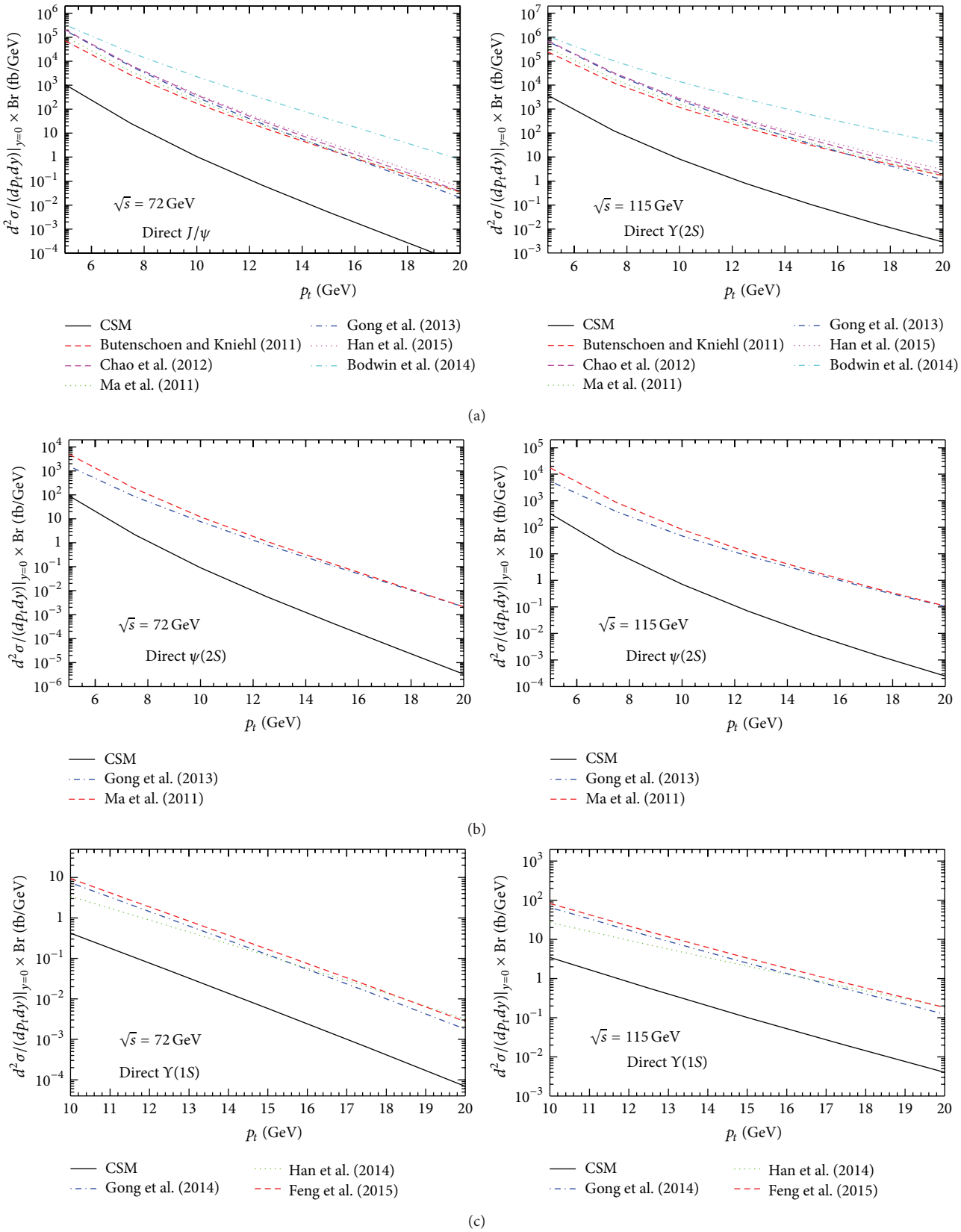

FIGURE 3: Transverse momentum distribution of differential cross section with the rapidity $y = 0$ for direct J/ψ, $\psi(2S)$, and $\Upsilon(1S)$ hadroproduction from (a) to (c), respectively.

that charmonium yields can easily reach 10^9 per year and 10^6 for bottomonium at the center of mass energy $\sqrt{s} \simeq 115$ GeV in pp collision.

Conflict of Interests

The authors declare that there is no conflict of interests regarding the publication of this paper.

Acknowledgment

The authors are grateful to Jean-Philippe Lansberg for his generous help in this work.

References

[1] G. T. Bodwin, E. Braaten, and G. P. Lepage, "Rigorous QCD analysis of inclusive annihilation and production of heavy quarkonium," *Physical Review D*, vol. 51, no. 3, pp. 1125–1171, 1995.

[2] Y.-Q. Ma, K. Wang, and K.-T. Chao, "$J/\psi(\psi')$ Production at the Tevatron and LHC at $\mathcal{O}(\alpha_s^4 v^4)$ in Nonrelativistic QCD," *Physical Review Letters*, vol. 106, Article ID 042002, 2011.

[3] M. Butenschoen and B. A. Kniehl, "Reconciling J/ψ production at HERA, RHIC, tevatron, and LHC with nonrelativistic QCD factorization at next-to-leading order," *Physical Review Letters*, vol. 106, Article ID 022003, 2011.

[4] M. Butenschoen and B. A. Kniehl, "J/ψ polarization at the Tevatron and the LHC: nonrelativistic-QCD factorization at the crossroads," *Physical Review Letters*, vol. 108, Article ID 172002, 2012.

[5] K.-T. Chao, Y.-Q. Ma, H.-S. Shao, K. Wang, and Y.-J. Zhang, "J/ψ polarization at Hadron colliders in nonrelativistic QCD," *Physical Review Letters*, vol. 108, Article ID 242004, 2012.

[6] B. Gong, L.-P. Wan, J.-X. Wang, and H.-F. Zhang, "Polarization for prompt J/ψ and $\psi(2s)$ production at the Tevatron and LHC," *Physical Review Letters*, vol. 110, Article ID 042002, 2013.

[7] K. Wang, Y.-Q. Ma, and K.-T. Chao, "$\Upsilon(1S)$ prompt production at the Tevatron and LHC in nonrelativistic QCD," *Physical Review D*, vol. 85, Article ID 114003, 2012.

[8] B. Gong, L.-P. Wan, J.-X. Wang, and H.-F. Zhang, "Complete next-to-leading-order study on the yield and polarization of $\Upsilon(1S, 2S, 3S)$ at the Tevatron and LHC," *Physical Review Letters*, vol. 112, Article ID 032001, 2014.

[9] Y. Feng, J.-P. Lansberg, and J.-X. Wang, "Energy dependence of direct-quarkonium production in pp collisions from fixed-target to LHC energies: complete one-loop analysis," http://arxiv.org/abs/1504.00317.

[10] S. J. Brodsky, F. Fleuret, C. Hadjidakis, and J. P. Lansberg, "Physics opportunities of a fixed-target experiment using LHC beams," *Physics Reports*, vol. 522, no. 4, pp. 239–255, 2013.

[11] J. P. Lansberg, S. J. Brodsky, F. Fleuret, and C. Hadjidakis, "Quarkonium physics at a fixed-target experiment using the LHC beams," *Few-Body Systems*, vol. 53, no. 1-2, pp. 11–25, 2012.

[12] L. Massacrier, M. Anselmino, R. Arnaldi et al., "Studies of transverse-momentum-dependent distributions with A Fixed-Target ExpeRiment using the LHC beams (AFTER@LHC)," http://arxiv.org/abs/1502.00984.

[13] J. P. Lansberg, M. Anselmino, R. Arnaldi et al., "Spin physics and TMD studies at a fixed-target experiment at the LHC (AFTER@LHC)," *EPJ Web of Conferences*, vol. 85, Article ID 02038, 2015.

[14] A. Rakotozafindrabe, R. Arnaldi, S. Brodsky et al., "Ultra-relativistic heavy-ion physics with AFTER@LHC," *Nuclear Physics A*, vol. 904-905, pp. 957c–960c, 2013.

[15] P. L. Cho and A. K. Leibovich, "Color-octet quarkonia production. II," *Physical Review D*, vol. 53, pp. 6203–6217, 1996.

[16] B. Harris and J. Owens, "Two cutoff phase space slicing method," *Physical Review D*, vol. 65, Article ID 094032, 2002.

[17] B. Gong and J.-X. Wang, "QCD corrections to polarization of J/ψ and Υ at Fermilab Tevatron and CERN LHC," *Physical Review D*, vol. 78, Article ID 074011, 2008.

[18] B. Gong, X. Q. Li, and J.-X. Wang, "QCD corrections to J/ψ production via color-octet states at the Tevatron and LHC," *Physics Letters B*, vol. 673, no. 3, pp. 197–200, 2009.

[19] B. Gong, J.-X. Wang, and H.-F. Zhang, "QCD corrections to Υ production via color-octet states at the Tevatron and LHC," *Physical Review D*, vol. 83, Article ID 114021, 2011.

[20] J.-X. Wang, "Progress in FDC project," *Nuclear Instruments and Methods in Physics Research Section A: Accelerators, Spectrometers, Detectors and Associated Equipment*, vol. 534, no. 1-2, pp. 241–245, 2004.

[21] E. J. Eichten and C. Quigg, "Quarkonium wave functions at the origin," *Physical Review D*, vol. 52, pp. 1726–1728, 1995.

[22] M. Butenschoen and B. A. Kniehl, "World data of J/ψ production consolidate nonrelativistic QCD factorization at next-to-leading order," *Physical Review D*, vol. 84, Article ID 051501, 2011.

[23] H.-F. Zhang, Z. Sun, W.-L. Sang, and R. Li, "Impact of η_c hadroproduction data on charmonium production and polarization within the nonrelativistic QCD framework," *Physical Review Letters*, vol. 114, Article ID 092006, 2014.

[24] H. Han, Y.-Q. Ma, C. Meng, H.-S. Shao, and K.-T. Chao, "η_c production at LHC and implications for the understanding of J/ψ production," *Physical Review Letters*, vol. 114, Article ID 092005, 2015.

[25] G. T. Bodwin, H. S. Chung, U.-R. Kim, and J. Lee, "Fragmentation contributions to J/ψ production at the Tevatron and the LHC," *Physical Review Letters*, vol. 113, Article ID 022001, 2014.

[26] H. Han, Y.-Q. Ma, C. Meng, H.-S. Shao, and Y.-J. Zhang, 1410.8537,2014.

[27] Y. Feng, B. Gong, L.-P. Wan, and J.-X. Wang, "An updated study for Υ production and polarization at the Tevatron and LHC," http://xxx.tau.ac.il/abs/1503.08439.

[28] J. Pumplin, D. Stump, J. Huston, H.-L. Lai, P. M. Nadolsky, and W.-K. Tung, "New generation of parton distributions with uncertainties from global QCD analysis," *Journal of High Energy Physics*, vol. 2002, no. 7, article 12, 2002.

[29] K. Olive, K. Agashe, C. Amsler et al., "Review of particle physics," *Chinese Physics C*, vol. 38, Article ID 090001, 2014.